ISBN: 978-3-95450-224-0 ISSN: 2673-7035 doi:10.18429/JACoW-FLS2023-WE4P31

DETERMINISTIC LATTICE APPROACH FOR BESSY III*

B. Kuske†, P. Goslawski, Helmholtz-Zentrum Berlin, Berlin, Germany

Abstract

Since 2021, HZB pursues the design of a 2.5 GeV storage ring as a successor of BESSY II in Berlin. The user's demand for diffraction-limited radiation at 1 keV corresponds to an emittance of 100 pm, making an MBA lattice indispensable. The envisaged location limits the circumference to ≈350 m. MBA lattices are composed of smaller substructures that can be analyzed and optimized separately, before combining them into one super period. The prerequisite for this approach is a clear idea of the goal parameters and their prioritization, as the design process is dominated by permanent decisions between different options. The resulting generic baseline lattice for BESSY III is a simple structure with few non-linear elements, already fulfilling all goal parameters and showing a very compatible non-linear behavior. This is our starting point for further optimizations including swarm or MOGA approaches.

INTRODUCTION

Multi-bend achromat lattices utilize many bending magnets with low deflection angles to reduce the emittance. Usually, these bends are placed at the center of repetitive unit cells, UCs. Multi-bend achromat lattices were pioneered by MAX LAB, Sweden. MAX IV, [1], was successfully commissioned in 2016. Sirius in Brazil followed in 2021, [2]. The ESRF, France, followed with the hybrid MBA in 2021, [3]. Nowadays, practically every new machine design or upgrade utilizes this type of lattice.

In 2014, A. Streun, PSI, added the concept of reverse bends (RB) to the MBA unit cell, UC, [4]. RBs are focusing quadrupoles placed off-axis to achieve negative bending. They detach the dispersion- and beta-function matching and significantly reduce the emittance.

In 2017, J. Bengtsson contributed the Higher-Order-Achromat approach to MBA-lattices [5, 6], where the linear lattice is constructed such, that all 1st and 2nd order resonance driving terms are suppressed by phase cancellation.

HZB now proposes a deterministic lattice design approach based on both, RB and HOA. The repetitive structure of MBA lattices is exploited to optimize small substructures, the UC, the dispersion suppression cell (DSC), and the straight section separately before they are composed into one generic super period. An important goal is to minimize non-linear effects by the set-up of the linear lattice structure. This approach leads to lattices close to the achievable optimum under the given boundary conditions, including fundamental decisions on a promising sextupole scheme. Opposed to generic optimizations this approach leads to a clear understanding of the parameter space and optional trade-offs.

An indispensable prerequisite of this approach is a clear definition of the design goals and their priorities. For BESSY III [7], these are listed in Tables 1 and 2.

Table 1: BESSY III Goal Parameters

Parameter	Value
Energy	2.5 GeV
Super Periods	16
Circumference	≈350 m
Emittance	100 pm
Momentum Compaction Factor, α_c	> 1e-4
Momentum Acceptance	> 3 %

Table 2: Design Priorities

	Goal	Reason
1	MBA lattice	emittance
1	realization of HOA	non-linear behaviour
1	usage of reverse bends	emittance, circumference
2	low sextupole strength	non-linear behaviour
2	short circumference	site, costs
3	DSC as close as possible to half UC	non-linear behaviour

CONSTRUCTION OF THE UC

The half UC minimally consists of a central, main bend, MB, the reverse bend, RB, the defocusing quadrupole, QD, and 2 sextupoles, SF and SD. Initially, all drifts are 0.1 m.

HOA Condition for UC

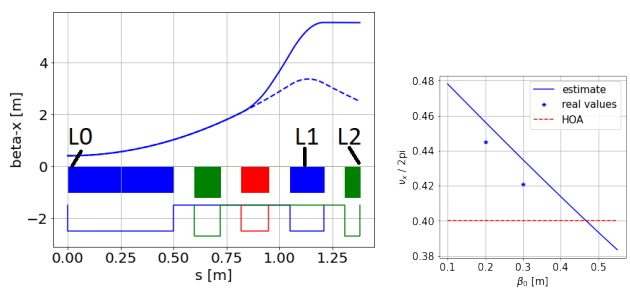

Figure 1: Left: β_x in half UC, regular (line) and for QD=0 (dashed line); magnet color code: MB: blue; RB: purple; QD: red, SF, SD: green. Right: ν_x, analytic estimate (blue line), exact phase advance (stars), and option for HOA (red).

* Work supported by German Bundesministerium für Bildung und Forschung, Land Berlin, and grants of Helmholtz Association
† Bettina.Kuske@helmholtz-berlin.de

ISBN: 978-3-95450-224-0 ISSN: 2673-7035 doi:10.18429/JACoW-FLS2023-WE4P31

The HOA condition on the phase advances $\nu_{x,y}$ in the UC is given by $n \cdot \nu_{x,y} = N$, where n is the number of UC in the arc and N is a lower integer. An upper limit for the horizontal phase advance in the UC is given for zero vertical focusing, QD = 0. β_x then develops like in a drift space from the center of the MB, β_0 at s=0, to β_1 at s=L1, at the RB. It can be assumed constant to the end of the UC at s=L2, see Fig. 1, left. An upper limit for ν_x is then given by

$$\nu_x < \int_0^{L1} \frac{\beta_0}{\beta_0^2 + s^2} ds + \int_{L1}^{L2} \frac{1}{\beta_1} = \arctan\left(\frac{L_1}{2\pi\beta_0}\right) + \frac{L_2 - L_1}{2\pi\beta_1}$$

Figure 1, right, shows this estimate for a wide range of β_0. The only option in this range to fulfill the HOA condition in the horizontal plane is indicated by the red line: $5 \cdot 0.4 = 2$.

Emittance Minimization

For fixed dipole parameters, the emittance is determined by β_0, η_0, at the center of the UC and the damping partition number, J_x. In the HOA-UC, β_0 is determined by the horizontal phase advance. For fixed phase advance, η_0 is determined by the RB angle. The bending gradients (MB and RB) determine the damping partition number, J_x.

$$J_x = 1 - \frac{I4}{I2} = 1 - \frac{\int_0^C \frac{\eta_x}{\rho^3} + \frac{2k\eta_x}{\rho}}{\int_0^C \frac{1}{\rho^2}} ds$$

Clearly, k and η_x at the RB are much larger than at the MB, while the bending radius, ρ, is in the same order of magnitude.

Figure 2 shows the impact on the damping partition number (left) and on the emittance (right) of a gradient in the MB (blue line) and that of an angle of the RB (green line), starting from a homogeneous bend and a pure focusing quadrupole. In all cases, the UC is fitted to phase advances of $\nu_{x,y}/2\pi = 0.4, 0.1$.

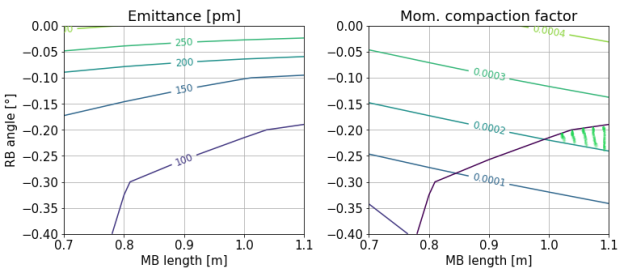

Figure 2: Left: J_x as a function of the MB gradient, blue, and the RB angle, green. Right: emittance for the same cases. Dashed line: $\epsilon * J_x$, i.e. the effect of the changing β-functions.

The much larger emittance reduction by the RB is caused by its superior β-functions and the larger gradient. Combining both effects, the gradient in the MB would worsen these conditions and enlarge the emittance. Therefore, the utilization of an RB is a better choice than a gradient MB.

The length of the MB (for fixed angle), also impacts the emittance, as well as the momentum compaction factor, α_c. Figure 3 shows the emittance (left) and α_c (right) as a function of the RB angle and the length of MB for a fixed deflection angle. The demand for an emittance of 100 pm sets clear limits for the RB angle, as well as for the dipole length. If, in addition, also $\alpha_c > 2 \cdot 10^{-4}$ is demanded for the UC (corresponding to $\alpha_c > 1 \cdot 10^{-4}$ for the complete lattice), only the green shaded area fulfills both design goals.

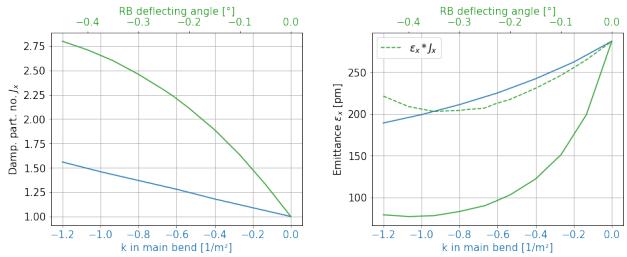

Figure 3: Left: emittance as a function of the RB angle and the MB length for fixed deflection angle. Right: α_c for the same cases.

Magnet Sorting and Angle Distribution

The different options for sorting the magnets in the UC have been discussed in [8]. There are 4 possible magnet configurations of the UC with a homogeneous MB, all similar in emittance and chromaticity, but very different, up to a factor of 2, in the sextupole strength needed to compensate for the chromaticity. The configuration with the least sextupole strength places the SD next to the main bend and the SF at the outside of the UC.

In [9] it has been shown, that the distribution of the deflection angle between the UC and the DSC is of minor importance with regard to the emittance and α_c. In an optimal configuration of both cells, only a few pm can be gained in the emittance.

Therefore, the position of the magnets and all important magnet parameters of the UC can be determined from the phase conditions of the HOA, the goal emittance and α_c, and the goal to keep non-linear fields low. This guarantees a solution, under the given boundary conditions, close to the optimum. For the resulting β-functions, a suitable DSC has to be developed.

CONSTRUCTION OF THE DISPERSION SUPPRESSION CELL

The optimal conditions to seek low emittance in the DSC have been discussed in [9]. The best practical results with regard to the non-linear behavior have been achieved by designing the DSC as close as possible to the UC, preserving the phase relation between the sextupoles. To this end, the suppression of the dispersion must be mainly achieved by variation of the dipole parameters, i.e. the reverse bend angle (and therefore the DSB-angle, to keep the total deflection) and the length of the final bend. Minor adjustments of the RB field can be used to achieve a flat vertical β_y-function. Figure 4 shows a typical result.

ISBN: 978-3-95450-224-0 ISSN: 2673-7035 doi:10.18429/JACoW-FLS2023-WE4P31

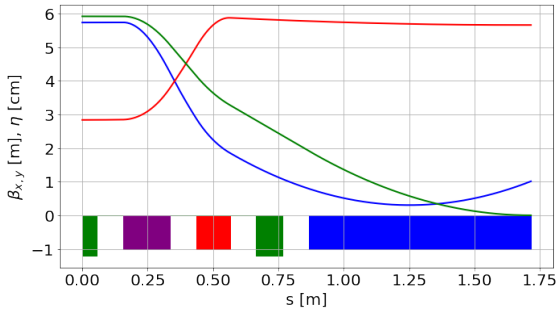

Figure 4: Typical DSC with dispersion suppression using mainly dipole parameters. β_x: blue, β_y: red, η_x: green. Magnet color code as above.

MATCHING THE STRAIGHT SECTION

The Twiss parameters at the end of the DS-bend must now be matched to the center of the straight section. A simple scan over doublet-, triplet- or quadruplet solutions can seek an overview of the options for matching. For BESSY III the design goal is 3 m β-functions in both planes at the center of the straight section with a length of 5.6 m. The only possible matching was achieved using 4 quadrupoles. The exact value of the β-functions is later sacrificed to achieve the desired working point, without changing the optimized UC and DSC parameters.

NON-LINEAR ASPECTS

The non-linear behavior of a lattice is governed by the resonance driving terms. One of the goals of the design process was to keep the unavoidable chromatic sextupole strength as low as possible, as the terms of the geometric as well as the amplitude-dependent driving terms include the integrated sextupole strength. Low sextupole fields keep the necessary higher-order corrections low.

The sum of the absolute chromatic sextupole strength can be calculated and compared to the achieved emittance, normalized by the square of the energy. For rough orientation, Table 3 compares the chromatic sextupole strength for a few cases. The necessary chromatic sextupole strength of BESSY III lies only 10 % over that of MAX 4, despite the much lower emittance, and is ≈70 % of that of SLS 2. Of course, a green field design has the advantage of not being limited by an existing beamline geometry and tunnel.

The periodicity of phase advance between the sextupole is disrupted due to the straight section. Therefore it makes sense to allow for some variation in the sextupole strength. Different schemes of grouping the chromatic schemes can be realized. Usually, the best results are reached by separating the sextupoles in the DSC. In order to get a realistic estimate of the momentum acceptance and the dynamic aperture without immense tracking effort, only momenta and amplitudes that correspond to a tune shift smaller than |0.1| in both planes are considered stable, resulting in minor reductions when tracking with errors. Figure 5 shows the difference in momentum acceptance (left) and in dynamic aperture (right) between a symmetric scheme with 2 chromatic sextupole families and with different settings in the DSC.

Table 3: Chromatic Sextupole Strength

	ε pm	E GeV	ε/E^2 pm/GeV²	$\Sigma(b_3 * L)$ 1/m²
MAX 4	336	3.0	37.3	5180
SLS 2	123	2.4	21.4	8148
BESSY III	99	2.5	15.8	5742
Soleil	81	2.75	10.7	20278

There is a 5 % increase in momentum acceptance and the dynamic aperture is almost doubled. Separation into different families of the chromatic sextupoles is one of the most efficient knobs to improve the non-linear behavior of the lattice.

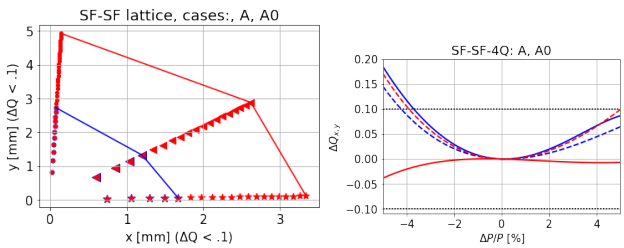

Figure 5: left: tune shift with momentum, 3.8 % for 2 families of chromatic sextupoles (blue) and 4.0 % with 4 families (red); right: dynamic aperture for the same cases, ΔQ < |0.1|

CONCLUSION

HZB introduces a design procedure for MBA lattices, that develops the lattice in a deterministic way, rather than using resource-intensive optimizers. By applying the insights of the HOA and the reverse bend, and trying to minimize the sextupole fields, the unit cell is fixed to a large extent. The dispersion suppression cell is designed as close as possible to the unit cell. The mapping of the boundary conditions of the DSC onto the conditions at the center of the straight section is only possible with 4 quadrupoles in BESSY III. The resulting sextupole strength is small, and even without additional harmonic sextupoles or octupoles, the design criteria for the momentum acceptance can be exceeded. The lattice needs a modified injection straight with an increased β_x-function unless vertical injection is considered.

This lattice is considered a baseline lattice. From here optimizations including the introduction of further non-linear components like harmonic sextupoles or octupoles, technical adaptions, and computer-based optimization schemes will be applied for further improvements. Due to the well-optimized starting point, this process is expected to be fast.

A further advantage of this approach is, that it provides knowledge of the interplay between different parameters and the trade-offs for pushing certain parameters to the limit. Contrary to common practice, it turned out that combined function magnets are not the best choice for MBA lattices, as long as reverse bends can be utilized.

ISBN: 978-3-95450-224-0 ISSN: 2673-7035 doi:10.18429/JACoW-FLS2023-WE4P31

REFERENCES

[1] S. Leemann *et al.*, "Beam dynamics and expected performance of Sweden's new storage-ring light source: MAX IV", *Phys. Rev. Spec. Top. Accel. Beams*, vol. 12, p. 120701, 2009. doi:10.1103/PhysRevSTAB.12.120701

[2] L. Liu *et al.*, "Preliminary Sirius commissioning results", in *11th Int. Particle Accelerator Conf. (IPAC'20)*, Caen, France, May 2020, paper MOVIR06. doi:10.18429/JACoW-IPAC2020-MOVIR06

[3] S. White, *et al.,* "Commissioning and restart of ESRF-EBS", in *Proc. 12th Int. Particle Accelerator Conf. (IPAC'21)*, Campinas, Brasil, May 2021, paper MOXA01. doi:10.18429/JACoW-IPAC2021-MOXA01

[4] A. Streun, "The anti-bend cell for ultralow emittance storage ring lattices", *Nucl. Instrum. Methods Phys. Res., Sect. A*, vol. 737, pp. 148–154, 2014. doi:10.1016/j.nima.2013.11.064

[5] J. Bengtsson and A. Streun, "Robust design strategy for SLS-2", Paul Scherrer Institut, Villigen, Switzerland, SLS2-BJ84-001-2, Jun. 2017.

[6] J. Bengtsson, "The sextupole scheme for the Swiss light source (SLS): An Analytical Approach", Paul Scherrer Institut, Villigen, Switzerland, SLS note 9-97, Mar. 1997.

[7] P. Goslawski *et al.*, "A highly competitive non-standard lattice for a 4th generation light source with metrology and timing capabilities", in *Proc. 67th ICFA Advanced Beam Dynamics Workshop on Future Light Sources (FLS'23)*, Lucerne, Switzerland, Aug. 2023, paper TU1B1, this conference.

[8] B. Kuske, M. Abo-Bakr, and P. Goslawski, "Basic design choices for the BESSY III MBA lattice", in *Proc. 13th Int. Particle Accelerator Conf. (IPAC'22)*, Bangkok, Thailand, Jun. 2022, paper MOPOTK009. doi:10.18429/JACoW-IPAC2022-MOPOTK009

[9] B. Kuske and P. Goslawski, "Further aspects of the deterministic lattice design approach for BESSY III", in *Proc. 14th Int. Particle Accelerator Conf. (IPAC'23)*, Venice, Italy, May 2023, paper WEPL039, to appear in the proceedings.